


RESEARCH ARTICLE

Open Access



Global neuropathologic severity of Alzheimer's disease and locus coeruleus vulnerability influences plasma phosphorylated tau levels

Melissa E. Murray^{1*} , Christina M. Moloney¹, Naomi Kouri¹, Jeremy A. Syrjanen², Billie J. Matchett¹, Darren M. Rothberg¹, Jessica F. Tranovich¹, Tiffany N. Hicks Sirmans¹, Heather J. Wiste², Baayla D. C. Boon¹, Aivi T. Nguyen³, R. Ross Reichard³, Dennis W. Dickson¹, Val J. Lowe⁴, Jeffrey L. Dage⁵, Ronald C. Petersen⁶, Clifford R. Jack Jr⁴, David S. Knopman⁶, Prashanthi Vemuri⁴, Jonathan Graff-Radford⁶ and Michelle M. Mielke^{2,7,8*}

Abstract

Background: Advances in ultrasensitive detection of phosphorylated tau (p-tau) in plasma has enabled the use of blood tests to measure Alzheimer's disease (AD) biomarker changes. Examination of postmortem brains of participants with antemortem plasma p-tau levels remains critical to understanding comorbid and AD-specific contribution to these biomarker changes.

Methods: We analyzed 35 population-based Mayo Clinic Study of Aging participants with plasma p-tau at threonine 181 and threonine 217 (p-tau181, p-tau217) available within 3 years of death. Autopsied participants included cognitively unimpaired, mild cognitive impairment, AD dementia, and non-AD neurodegenerative disorders. Global neuropathologic scales of tau, amyloid- β , TDP-43, and cerebrovascular disease were examined. Regional digital pathology measures of tau (phosphorylated threonine 181 and 217 [pT181, pT217]) and amyloid- β (6F/3D) were quantified in hippocampus and parietal cortex. Neurotransmitter hubs reported to influence development of tangles (nucleus basalis of Meynert) and amyloid- β plaques (locus coeruleus) were evaluated.

Results: The strongest regional associations were with parietal cortex for tau burden (p-tau181 $R=0.55$, $p=0.003$; p-tau217 $R=0.66$, $p<0.001$) and amyloid- β burden (p-tau181 $R=0.59$, $p<0.001$; p-tau217 $R=0.71$, $p<0.001$). Linear regression analysis of global neuropathologic scales explained 31% of variability in plasma p-tau181 (Adj. $R^2=0.31$) and 59% in plasma p-tau217 (Adj. $R^2=0.59$). Neither TDP-43 nor cerebrovascular disease global scales independently contributed to variability. Global scales of tau pathology (β -coefficient = 0.060, $p=0.016$) and amyloid- β pathology (β -coefficient = 0.080, $p<0.001$) independently predicted plasma p-tau217 when modeled together with co-pathologies, but only amyloid- β (β -coefficient = 0.33, $p=0.021$) significantly predicted plasma p-tau181. While nucleus

*Correspondence: murray.melissa@mayo.edu; mmielke@wakehealth.edu

¹ Department of Neuroscience, Mayo Clinic Florida, 4500 San Pablo Road, Jacksonville, FL 32224, USA

⁸ Department of Epidemiology and Prevention, Division of Public Health Sciences, Wake Forest University School of Medicine, 525 Vine, 5th floor, Winston-Salem, NC 27157, USA

Full list of author information is available at the end of the article



© The Author(s) 2022. **Open Access** This article is licensed under a Creative Commons Attribution 4.0 International License, which permits use, sharing, adaptation, distribution and reproduction in any medium or format, as long as you give appropriate credit to the original author(s) and the source, provide a link to the Creative Commons licence, and indicate if changes were made. The images or other third party material in this article are included in the article's Creative Commons licence, unless indicated otherwise in a credit line to the material. If material is not included in the article's Creative Commons licence and your intended use is not permitted by statutory regulation or exceeds the permitted use, you will need to obtain permission directly from the copyright holder. To view a copy of this licence, visit <http://creativecommons.org/licenses/by/4.0/>. The Creative Commons Public Domain Dedication waiver (<http://creativecommons.org/publicdomain/zero/1.0/>) applies to the data made available in this article, unless otherwise stated in a credit line to the data.

basalis of Meynert neuron count/mm² was not associated with plasma p-tau levels, a lower locus coeruleus neuron count/mm² was associated with higher plasma p-tau181 ($R = -0.50$, $p = 0.007$) and higher plasma p-tau217 ($R = -0.55$, $p = 0.002$). Cognitive scores (Adj. $R^2 = 0.25$ – 0.32) were predicted by the global tau scale, but not by the global amyloid- β scale or plasma p-tau when modeled simultaneously.

Conclusions: Higher soluble plasma p-tau levels may be the result of an intersection between insoluble deposits of amyloid- β and tau accumulation in brain, and may be associated with locus coeruleus degeneration.

Keywords: Alzheimer's Disease, Neuropathology, Blood biomarker, Phosphorylated Tau, Neurofibrillary Tangles, Amyloid- β , Digital Pathology

Background

Recent advances in technology have enabled ultrasensitive detection of plasma-derived phosphorylated-tau (p-tau) levels as a potential minimally-invasive Alzheimer's disease (AD) biomarker [1–4]. Plasma p-tau levels could provide a more feasible AD biomarker than neuroimaging or lumbar puncture at the population level for diagnosis or screening purposes [2]. Postmortem validation of antemortem plasma p-tau changes is critical for understanding the strength of the relationship between neuropathology and plasma p-tau levels, and thus, translation to the clinic [2, 5]. Autopsy series have demonstrated higher plasma p-tau levels in patients with AD dementia, compared to non-AD dementias, and high accuracy for predicting AD dementia [6–8]. Interestingly, non-disease controls and non-AD cases were shown to not differ in plasma p-tau levels, suggesting an AD-specific biomarker increase even when comparing to other tauopathies [1, 9, 10].

Comparison of plasma p-tau at threonine 181 (p-tau181) and threonine 217 (p-tau217) levels with brain-derived global tau scales provides important insight into neuropathologic temporality and individual variability [4, 11]. Neuroimaging studies suggest plasma p-tau levels reliably predict in vivo positron emission tomography (PET) assessments of both tau and amyloid- β [1, 8], but the correlation with amyloid- β may be stronger – especially in individuals with elevated amyloid- β PET measures (i.e. amyloid-PET positive) [3]. The stronger relationship in amyloid-PET positive individuals could be an inferred reflection of greater tau pathology in brain or an amyloid- β -specific neuronal reaction influencing soluble p-tau production [12, 13]. Thus, to inform clinical interpretation we investigated the contribution of tau and amyloid- β neuropathology to plasma p-tau181 and p-tau217 levels and identified whether other sources of variability contribute to plasma p-tau levels. As plasma p-tau levels are derived from circulating blood, we hypothesized that global scales of neuropathology would demonstrate a stronger association with plasma p-tau levels compared to regional measures digitally quantified from the hippocampus or parietal cortex. We further

assessed the impact of medical comorbidities [14] and common co-existing pathologies in the aging brain, including cerebrovascular disease [15] and TAR DNA binding protein 43 (TDP-43) [16], on plasma p-tau levels. Our overall goal was to examine clinicopathologic contributors to plasma p-tau181 and p-tau217 levels using global scales and regional measures to uncover sources of variability to help inform interpretation in the context of aging and neurodegeneration.

Methods

Participants

The Mayo Clinic Study of Aging (MCSA) is a population based, prospective study of residents living in Olmsted County, Minnesota. MCSA participants aged 70–89 were enumerated from the Rochester Epidemiology Project (REP) medical records-linkage system in 2004 and recruitment was extended in 2012 to participants aged 50 and older [17]. MCSA visits included an interview by a study coordinator, physician examination, cognitive testing, and a blood draw completed on the same day. The inclusion criteria for this study were MCSA participants who had undergone autopsy and who had plasma p-tau181 and p-tau217 levels within 3 years of death. To assess the relationship between neuropathology and cognition, Clinical Dementia Rating (CDR) [18] and Mini-Mental State Examination (MMSE) [19] were evaluated if testing occurred within 3 years of death.

Procedures

Blood was collected in-clinic after an overnight fast. The blood was centrifuged, resulting plasma aliquoted, and stored at -80°C . Both p-tau181 and p-tau217 levels were measured in duplicate on a streptavidin small spot plate using the meso scale discovery (MSD) platform by electrochemiluminescence using proprietary assays developed by Lilly Research Laboratories, as previously described [20]. Levels of creatinine, alanine transaminase (ALT), and aspartate aminotransferase (AST) were abstracted from the medical records at the time closest to the MCSA visit with the blood draw for the p-tau levels. Only serum creatinine (mg/dL), ALT (U/L), and AST

(U/L) levels identified within 3 years of the plasma p-tau blood draw were abstracted.

Neuropathologic sampling followed Consortium to Establish a Registry for Alzheimer's Disease (CERAD) recommendations and National Institute on Aging-Alzheimer's Association criteria for AD neuropathologic change assessment [21, 22]. Formalin-fixed, paraffin-embedded 5- μ m-thick tissue sections were stained with hematoxylin and eosin, as well as Bielschowsky silver stain. Immunohistochemistry was performed on a Thermo Fisher Lab Vision 480S autostainer with 3,3-diaminobenzidine as chromogen. Antibodies against tau, amyloid- β , α -synuclein, and TDP-43 were used for neuropathologic evaluation (Table S1) [22–24]. Cases were also evaluated for global scales that included Braak stage, Thal phase, limbic-predominant age-related TDP-43 encephalopathy neuropathologic change (LATE-NC), and Kalaria cerebrovascular disease score [15, 16, 25, 26]. Diffuse plaques and neuritic plaques were evaluated using a 4-point semi-quantitative scale: none, mild, moderate, and severe. Neuropathologic diagnoses were rendered by two board-certified neuropathologists (RRR and ATN). Neuropathologic grouping for graphical visualization was prioritized as follows: progressive supranuclear palsy ($n=2$) [27], AD ($n=9$) [22], argyrophilic grain disease ($n=3$) [28], primary age-related tauopathy ($n=14$) [29], and pathological aging ($n=7$) [30, 31] (Fig. S1). Participants were assigned the neuropathologic diagnosis of AD if they had a Braak stage \geq IV and had at least moderate neuritic plaques. Primary age-related tauopathy was assigned if they had a Braak stage \leq IV and Thal phase \leq 2. As part of ongoing efforts to investigate AD biomarkers [32, 33], we next assigned pathological aging if they had a Braak \leq III and at least moderate diffuse plaques with no more than moderate neuritic plaques. During evaluation of antemortem contributors to plasma p-tau variability, a single outlier argyrophilic grain disease case was identified that was excluded from subsequent correlation and modeling analyses of neuropathology and cognition.

To clarify nomenclature when describing phosphorylated tau, "p-tau" is used for biomarker levels and "pT" for neuropathologic burden. The terms neuropathology and pathology are exclusively used when referencing examination of brain tissue and not used in reference to plasma p-tau biomarker changes. Digital pathology was used to quantify histopathologic burden of tau (pT181, pT217) and amyloid- β (6F/3D) in inferior parietal cortex and CA1-subiculum of hippocampus, as described in [Supplementary Methods](#) (Tables S2 and S3). The parietal cortex was chosen as a region affected by accumulation of tau pathology in advanced AD (Braak stage $>$ IV), but with limited involvement hypothesized to be influenced by

age-related tau pathology [29]. The CA1 and subiculum subsectors of the hippocampus were specifically chosen to enhance relevance to AD, as they are highly vulnerable to tau pathology in AD compared to CA2 involvement more readily observed in primary tauopathies and age-related tauopathies [34, 35]. Neurotransmitter hubs reported to influence development of neurofibrillary tangles (i.e., nucleus basalis of Meynert) and amyloid- β plaques (i.e., locus coeruleus) were additionally evaluated for neuronal count/mm² on hematoxylin and eosin using pattern recognition digital pathology software, as described in [Supplementary Methods](#) (Table S4, Fig. S2, S3 and S4).

Statistical analysis

The statistical analysis consisted of five parts: a descriptive summary table giving median (25th, 75th percentiles) for the variables included in our study, receiver operating characteristic (ROC) curves with corresponding area under the curves (AUC), scatter plots, Spearman correlations, and linear regression models. The ROC/AUC analysis was run to ascertain the ability of continuous plasma p-tau181 and p-tau217 levels to predict intermediate-to-high from none-to-low AD neuropathologic change. To perform this analysis, logistic regression models using the plasma markers and cognitive scores were individually run, and the predicted values from these models were used to create the ROC curves and compute the AUCs. We also computed confidence intervals for the AUCs using bootstrap resampling with 10,000 replicates. The latter three analysis methods were used to investigate the relationship between the various measures of neuropathology and plasma p-tau181 and p-tau217 as well as the relationship of other important factors (i.e., age, creatinine, etc.) with these plasma markers. In the linear models, the plasma markers served as the outcomes and β -coefficients, confidence intervals, and p -values were computed. All variables are shown for each model. Neuropathology variables were used as predictors and adjusted- R^2 values were computed. Global neuropathology variables used as predictors included Braak stage (tau), Thal phase (amyloid- β), LATE-NC (TDP-43), and Kalaria cerebrovascular disease score. Global scales of tau and amyloid- β provide information on the topographic distribution of pathology (i.e., presence), but may not reflect severity of pathology. To quantitatively assess tau and amyloid- β pathology in corticolimbic regions, digital pathology was employed to enable a wider range of severity to be measured. Thus, regional neuropathology variables used as predictors included pT181, pT217, and 6F3D quantitatively measured in CA1-subiculum of the hippocampus and parietal

cortex. The standard cutoff of $p < 0.05$ was used to determine statistical significance. All statistical analyses were performed with R version 3.6.2 (R Foundation for Statistical Computing, Vienna, Austria) and SAS version 9.4 (SAS Institute, Cary, NC).

Role of the funding source

The sponsors of this study had no role in study design, collection of data, analysis of data, interpretation of data, or writing of the report. The corresponding authors had full access to all the data in the study and

had final responsibility for the decision to submit for publication.

Results

Among the 35 autopsy cases, the median (interquartile range) age of death was 86 (81, 89) years, 20 were male (57%) and all self-identified as non-Hispanic white (Table 1). The median time from plasma draw to death was 2.0 (1.4, 2.3) years.

Table 1 Participant characteristics summary table by neuropathologic grouping

	PSP (n = 2)	AD (n = 9)	AGD (n = 2 ^a)	PART (n = 14)	PA (n = 7)
Age at plasma, years	80 (79,81)	87 (84,90)	89 (88,89)	81 (78,84)	79 (72,86)
Age at death, years	82 (81,83)	89 (86,92)	90 (90,91)	83 (81,86)	80 (74,88)
Postmortem interval, hours	4 (4,5)	13 (9,18)	20 (19,21)	20 (18,22)	14 (11,21)
Females	0 (0%)	4 (44%)	1 (50%)	8 (57%)	2 (29%)
APOE ε4 positivity	0 (0%)	4 (44%)	1 (50%)	2 (14%)	3 (43%)
Clinical Dementia Rating, 0–18	0.5 (0,1)	4 (0.5,7)	2 (1,3)	0 (0,0)	0 (0,0.5)
Mini-Mental State Examination, 0–30	29 (28,30)	23 (23,27)	28 (27,28)	28 (28,29)	28 (28,30)
Tau-PET parietal SUVr	n/a	1.2 (1.1,1.3)	n/a	1.0 (1.0,1.1)	1.1 (1.1,1.1)
Fluid levels					
MSD plasma p-tau181, pg/mL	1.6 (1.3,1.9)	3.4 (2.5,4.3)	1.7 (1.6,1.9)	1.2 (0.9,1.5)	1.3 (1.1,1.8)
MSD plasma p-tau217, pg/mL	0.25 (0.21,0.29)	0.69 (0.52,0.75)	0.18 (0.17,0.20)	0.15 (0.12,0.20)	0.19 (0.17,0.29)
Creatinine, mg/dL	1.0 (1.0,1.0)	1.2 (0.9,1.3)	1.4 (1.2,1.6)	1.0 (1.0,1.4)	1.1 (1.1,1.3)
ALT level, U/L	n/a	22 (15,24)	21 (21,21)	21 (18,27)	19 (18,47)
AST level, U/L	24 (21,27)	23 (19,29)	18 (15,20)	26 (23,31)	28 (22,49)
Global scales					
Braak stage, 0–VI	III (III, III)	IV (IV, V)	II (II, II)	II (II, III)	II (II, II)
0 I II III IV V VI, counts	0 0 0 2 0 0 0	0 0 0 0 5 3 1	0 0 2 0 0 0 0	1 3 4 5 1 0 0	0 2 4 1 0 0 0
Thal phase, 0–5	3 (3,3)	5 (4,5)	0.5 (0,1)	1 (1,2)	3 (3,4)
0 1 2 3 4 5, counts	0 0 0 2 0 0	0 0 0 2 2 5	1 1 0 0 0 0	3 6 5 0 0 0	0 0 0 4 3 0
Diffuse plaques, Moderate-Frequent	2 (100%)	9 (100%)	1 (50%)	3 (21%)	7 (100%)
Neuritic plaques, Moderate-Frequent	2 (100%)	9 (100%)	0 (0%)	1 (7%)	4 (57%)
LATE-NC stage, 0–3	0 (0,0)	1 (0,2)	1 (1,2)	0 (0,0)	0 (0,0)
Kalaria CVD score, 0–10	3 (3,3)	4 (3,5)	6 (5,6)	2 (2,4)	3 (2,5)
Regional measures					
Parietal pT181, %	0.27 (0.27,0.27)	0.64 (0.54,0.93)	0.27 (0.22,0.32)	0.17 (0.12,0.22)	0.11 (0.080,0.23)
Parietal pT217, %	0.46 (0.38,0.55)	0.63 (0.38,4.9)	0.22 (0.20,0.25)	0.080 (0.060,0.090)	0.11 (0.10,0.12)
Parietal amyloid-β, %	2.7 (2.5,3.0)	2.7 (2.0,4.6)	0.24 (0.16,0.32)	0.16 (0.10,0.46)	1.1 (0.43,1.5)
Hippocampal pT181, %	0.58 (0.41,0.74)	2.5 (1.9,3.9)	0.84 (0.51,1.2)	0.28 (0.18,0.34)	0.34 (0.16,0.38)
Hippocampal pT217, %	4.8 (3.0,6.6)	21 (10,28)	6.6 (3.5,9.7)	2.3 (0.34,3.7)	0.95 (0.67,2.7)
Hippocampal amyloid-β, %	0.36 (0.25,0.47)	0.64 (0.16,1.8)	0.050 (0.040,0.050)	0.050 (0.040,0.12)	0.11 (0.060,0.34)
LC neurons/mm ²	25 (18,33)	30 (22,33)	22 (22,22)	44 (38,52)	45 (39,52)
nbM neurons/mm ²	14 (11,17)	19 (14,19)	30 (26,35)	22 (17,27)	20 (15,29)

Data presented are median and interquartile range (25th,75th). ^aAGD case with high creatinine was not included. Acronyms: AD Alzheimer's disease, AGD Argyrophilic grains disease, ALT Alanine transaminase, AST Aspartate aminotransferase, CVD Cerebrovascular disease, CAA Cerebral amyloid angiopathy, LATE-NC Limbic-predominant age-related TDP-43 encephalopathy neuropathologic change, LC Locus coeruleus, MSD Meso scale discovery. p-tau phosphorylated tau in plasma, n/a not available, nbM nucleus basalis of Meynert, PA Pathological aging, PART Primary age-related tauopathy, PSP Progressive supranuclear palsy, pT phosphorylated threonine for immunohistochemical measures of tau

Antemortem contributors evaluated for contribution to plasma p-tau variability

As previous studies suggested that comorbidities, including both kidney and liver disease, may affect p-tau biomarker levels [14, 36], we first examined Spearman correlations of creatinine, AST, and ALT with plasma p-tau levels (Fig. S5). One individual was identified as an outlier with high serum creatinine (3.7 mg/dL) and the highest plasma p-tau levels (p-tau181 = 10 pg/mL, p-tau217 = 1.3 pg/mL). This individual remained part of the initial analyses evaluating antemortem variability of creatinine, AST, ALT, age at plasma p-tau draw, and time from blood draw to death. However, this individual was removed from subsequent analyses investigating neuropathology and cognition. AST and ALT were not found to significantly associate with plasma p-tau levels, which is further described in [Supplemental Results](#). We next examined the relationship between age at plasma p-tau draw and time from plasma draw to death with plasma p-tau levels (Fig. S5). Age at plasma draw did not correlate with plasma p-tau181 ($R=0.25$, $p=0.142$) or with plasma p-tau217 ($R=0.27$, $p=0.121$). Similarly, time from plasma to death did not correlate with plasma p-tau181 ($R=-0.012$, $p=0.947$) or with plasma p-tau217 ($R=-0.027$, $p=0.879$).

Qualitative global scales of neuropathology evaluated as predictors of plasma p-tau

We next assessed the relationship between global scales of AD neuropathologic change and plasma p-tau levels (Table 2). A discernible threshold of increase visibly appeared to be between Braak stage III and stage IV (Fig. 1A, C), corresponding with the observation of cortical tau pathology by Braak stage IV [25, 37]. Braak stage associated with both plasma p-tau181 ($R=0.45$, $p=0.008$) and plasma p-tau217 ($R=0.48$, $p=0.004$). Visual inspection of Thal phase graphs suggested a biological effect of increase between Thal phase 3 and phase 4 (Fig. 1B, D), corresponding with observations of amyloid- β plaque pathology in brainstem by Thal phase 4 [26]. While Thal phase strongly associated with plasma p-tau181 ($R=0.57$, $p<0.001$), the correlation was even stronger with plasma p-tau217 ($R=0.71$, $p<0.001$). Similarly, diffuse plaque scores (p-tau181 $R=0.44$, $p=0.009$; p-tau217 $R=0.64$, $p<0.001$) and neuritic plaque scores (p-tau181 $R=0.39$, $p=0.024$; p-tau217 $R=0.57$, $p<0.001$) were more strongly associated with plasma p-tau217 compared to p-tau181 (Table 2).

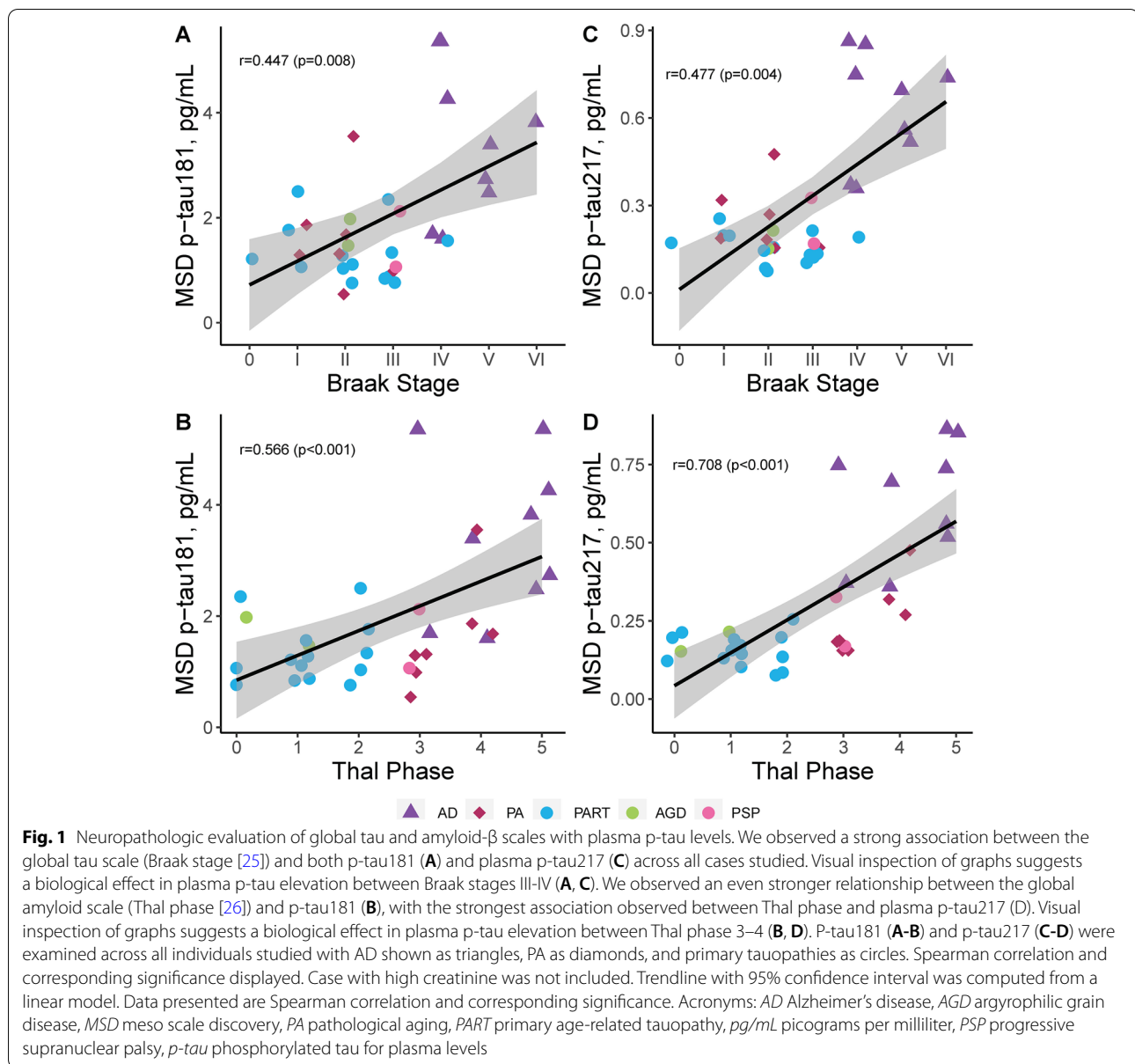
Based upon the surprising past [3, 38, 39] and current (Table 2) observations of a stronger association between amyloid- β in the brain and plasma p-tau, we

Table 2 Evaluation of the relationship between global scales and regional neuropathologic measures with plasma p-tau181 and p-tau217 levels

	MSD plasma p-tau181	MSD plasma p-tau217
Global scales	R (p-value)	R (p-value)
Braak stage	0.45 (0.008)	0.48 (0.004)
Thal phase	0.57 (<0.001)	0.71 (<0.001)
Diffuse plaques score	0.44 (0.009)	0.64 (<0.001)
Neuritic plaques score	0.39 (0.024)	0.57 (<0.001)
LATE-NC stage	0.13 (0.464)	0.16 (0.379)
Kalaria CVD score	0.32 (0.067)	0.27 (0.119)
Regional measures	R (p-value)	R (p-value)
Hippocampal pT181	0.37 (0.054)	0.43 (0.023)
Hippocampal pT217	0.30 (0.087)	0.28 (0.113)
Hippocampal 6F/3D	0.41 (0.018)	0.46 (0.007)
Parietal pT181	0.55 (0.003)	0.55 (0.003)
Parietal pT217	0.55 (<0.001)	0.66 (<0.001)
Parietal 6F/3D	0.59 (<0.001)	0.71 (<0.001)
LC neurons/mm ²	-0.50 (0.007)	-0.55 (0.002)
nbM neurons/mm ²	-0.10 (0.663)	-0.18 (0.418)

Spearman correlation data presented with correlation coefficient (R) and significance (p-value). Case with high creatinine was not included. Acronyms: CAA Cerebral amyloid angiopathy, CVD Cerebrovascular disease, LATE-NC Limbic-predominant age-related TDP-43 encephalopathy neuropathologic change, LC Locus coeruleus, MSD Meso scale discovery, nbM nucleus basalis of Meynert, p-tau phosphorylated tau in plasma, pT phosphorylated threonine for immunohistochemical measures of tau

sought to investigate the predictive relationship between neuropathologic variables as predictors and plasma p-tau levels as outcome. In consideration of the common observation of co-existing neuropathologies in the aging brain [15, 16, 40, 41], we included TDP-43 (LATE-NC [16]) and cerebrovascular disease (Kalaria score [15, 42]) in the regression model. Models were restricted to four predictors based upon sample size, but sensitivity analyses including time from plasma to death confirmed observations presented in Table S5. When examining global scales of neuropathology, 31% of the variability in p-tau181 was explained (Adj. $R^2=0.31$). Thal phase (β -coefficient = 0.33 [0.053, 0.60], $p=0.021$) was the main predictor of p-tau181. Neither Braak stage, LATE-NC stage, nor Kalaria cerebrovascular disease score contributed independently to p-tau181 levels. In contrast to p-tau181, global scales accounted for 59% of the variability in p-tau217 (Adj. $R^2=0.59$). Both Thal phase (β -coefficient = 0.080 [0.042, 0.12], $p<0.001$) and Braak stage (β -coefficient = 0.060 [0.012, 0.11], $p=0.016$) independently predicted p-tau217 levels, but LATE-NC stage or Kalaria cerebrovascular disease score did not.



Quantitative digital pathology measures evaluated as predictors of plasma p-tau

Multivariable regression analyses utilizing global scales of neuropathology provided further evidence that accumulating insoluble amyloid- β plaque pathology predicts higher soluble p-tau levels in plasma (Table S5). To further evaluate this perplexing relationship, quantitative regional measures of immunohistochemical burden of tau and amyloid- β using digital pathology were next evaluated in the CA1-subiculum hippocampal subsectors and parietal cortex (Table 2). The association of hippocampal burden with plasma p-tau181 was similar for tau pathology (pT181

$R = 0.37$, $p = 0.054$) and amyloid- β pathology (6F/3D $R = 0.40$, $p = 0.018$) (Fig. S6). However, the association of hippocampal burden with plasma p-tau217 was lower for tau pathology (pT217 $R = 0.28$, $p = 0.113$) than amyloid- β pathology (6F/3D $R = 0.46$, $p = 0.007$). The strength of the association of parietal cortex burden with plasma p-tau181 was robustly observed for both tau pathology (pT181 $R = 0.55$, $p = 0.003$; Fig. 2A) and amyloid- β pathology (6F/3D $R = 0.59$, $p < 0.001$; Fig. 2B). The strongest association observed between parietal cortex burden and plasma p-tau217 was for tau pathology (pT217 $R = 0.66$, $p < 0.001$; Fig. 2C)

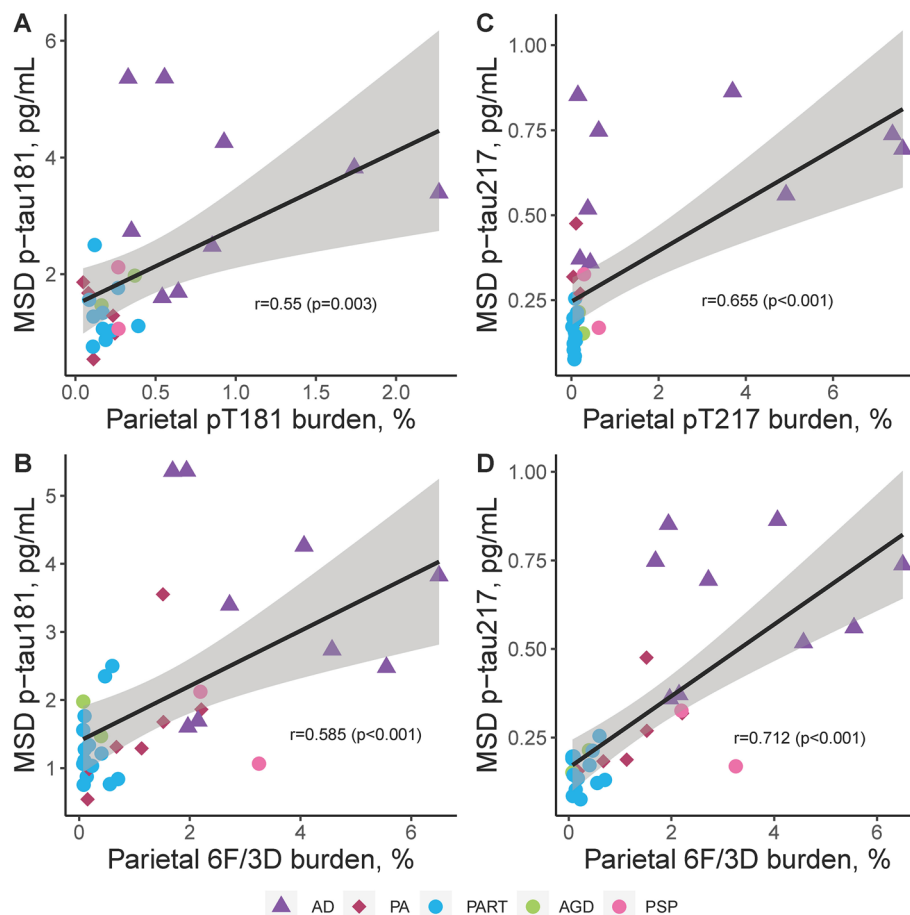


Fig. 2 Neuropathologic evaluation of regional digital pathology measures of tau and amyloid- β pathology in comparison to plasma p-tau181 and p-tau217 in parietal cortex. Utilizing the same epitope to immunohistochemically evaluate regional tau pathology in inferior parietal cortex, tau burden measures were compared to p-tau plasma levels (**A, C**). pT181 tau burden measures strongly associated with p-tau181 plasma levels (**A**), with the association even stronger between pT217 and p-tau217 plasma levels (**C**). Digital pathology measures of amyloid- β (6F/3D) were additionally compared to plasma p-tau levels (**B, D**). Amyloid- β burden strongly associated with ptau-181 (**B**). The strongest overall association of digital pathology measures was observed between amyloid- β (6F/3D) and p-tau217 (**D**). P-tau181 (**A-B**) and p-tau217 (**C-D**) were examined across all individuals studied with AD shown as triangles, PA as diamonds, and primary tauopathies as circles. Spearman correlation and corresponding significance displayed. Trendline with 95% confidence interval was computed from a linear model. Data presented are Spearman correlation and corresponding significance. Acronyms: AD Alzheimer's disease, AGD argyrophilic grain disease, MSD meso scale discovery, PA pathological aging, PART primary age-related tauopathy, PSP progressive supranuclear palsy, p-tau phosphorylated tau for plasma levels, pT phosphorylated threonine for immunohistochemical measures of tau

and amyloid- β pathology (6F/3D $R=0.71$, $p<0.001$; Fig. 2D).

To focus our investigation, we next performed linear modeling utilizing digital pathology burden measures derived from parietal cortex because this region was more strongly correlated with plasma p-tau levels compared to hippocampus (Table S5). Although the model for plasma p-tau181 accounted for 24% of the variability (Adj. $R^2=0.24$), neither parietal cortex pT181 tau burden, parietal cortex amyloid- β burden, LATE-NC stage, nor Kalaria cerebrovascular disease score significantly contributed when modeled together (Fig. 3). In contrast,

51% of the variability in p-tau217 (Adj. $R^2=0.51$) was accounted for by a similar model. Amyloid- β burden in the parietal cortex (β -coefficient=0.077 [0.026, 0.13], $p=0.004$) remained the main predictor of p-tau217, but there was not an independent contribution from parietal cortex pT217 tau burden, LATE-NC stage, or Kalaria cerebrovascular disease score.

Quantitative assessment of neurotransmitter hubs association with plasma p-tau

Based on the strength of the relationship observed between amyloid- β neuropathology and plasma p-tau

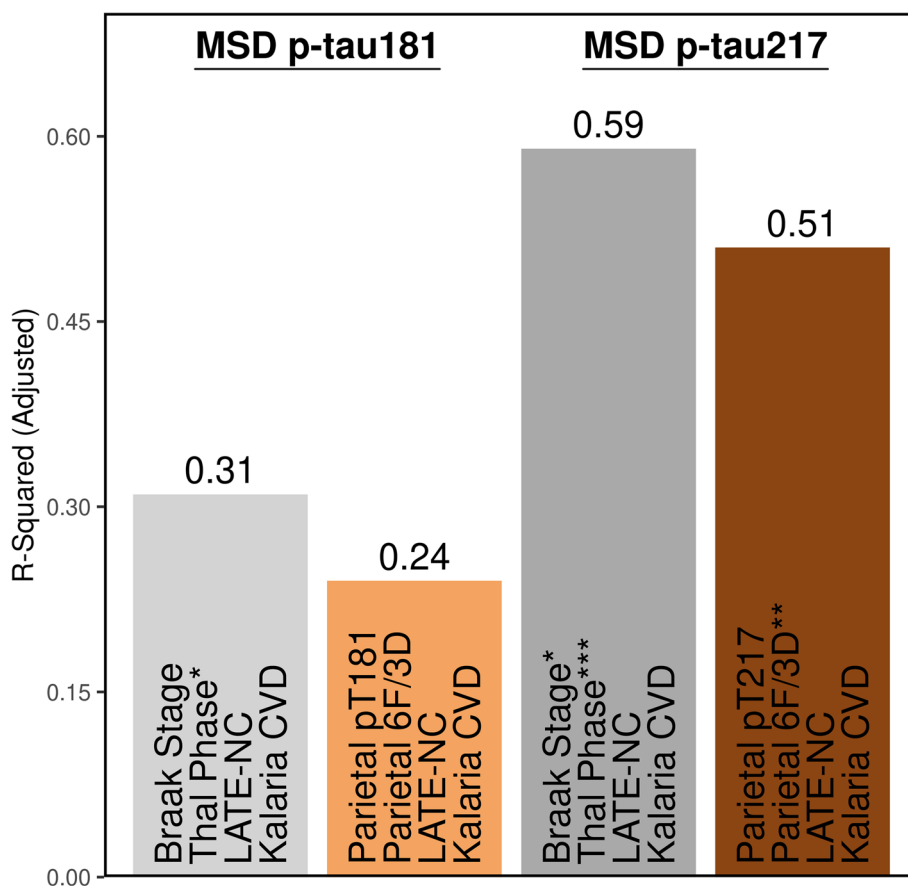


Fig. 3 Multivariable linear regression modeling of neuropathologic variables as predictors of plasma p-tau levels. Global scales of tau and amyloid- β (Braak [25] and Thal [26], gray bars) and the strongest regional measure of tau and amyloid- β (parietal cortex, brown bars) were investigated as predictors of variability observed in plasma p-tau181 (left) and p-tau217 levels (right). To account for common co-pathologies, LATE-NC [16] and Kalaria cerebrovascular disease [15] were added to each model. Overall, the global scales performed better than the regional cortical measures with amyloid- β observed as strongest contributor to plasma p-tau variability. Time from plasma draw to death was not used to adjust, as it was not observed to associate with plasma p-tau levels. Case with high creatinine was not included. All variables in the model are shown, corresponding to Table S5. Significance denoted as * $p < 0.05$, ** $p < 0.01$, *** $p < 0.001$. Acronyms: 6F/3D amyloid- β antibody, CVD cerebrovascular disease, LATE-NC limbic predominant age-related TDP-43 encephalopathy neuropathologic change, MSD meso scale discovery, p-tau phosphorylated tau for plasma levels, pT phosphorylated threonine for immunohistochemical measures of tau

levels (Table 2), along with the diminished relationship with Braak stage (Table S5), we next explored the neurotransmitter hubs considered to influence amyloid- β (locus coeruleus [43, 44]) and tau pathology (nucleus basalis of Meynert [45, 46]) through their widespread cortical projections. Nucleus basalis of Meynert neuron count/mm² was not associated with either plasma p-tau181 or plasma p-tau217 (Table 2, Fig. S7). In contrast, a lower locus coeruleus neuron count/mm² was strongly associated with higher plasma p-tau181 ($R = -0.50$, $p = 0.007$) and plasma p-tau217 ($R = -0.55$, $p = 0.002$).

Global neuropathologic scales and plasma p-tau evaluated as predictors of cognitive decline

Following assessment of antemortem and postmortem predictors of plasma p-tau variability, we examined the relationship between neuropathology and widely used cognitive measures (CDR [18], MMSE [19]) for generalizability. Based on consistent reports that plasma p-tau levels associated with cognitive decline [1, 3, 8, 9, 47, 48], we sought to investigate whether soluble measures of plasma p-tau independently predicted cognitive decline when accounting for insoluble measures of amyloid- β and tau pathology. To do this we performed linear regression analysis on CDR and MMSE assessed nearest the time of death (Table S6) while controlling for time from

plasma draw to death. Variability in cognitive scores was similarly predicted for CDR (p-tau181 model: Adj. $R^2=0.25$; p-tau217 model: Adj. $R^2=0.27$) and MMSE (p-tau181 model: Adj. $R^2=0.30$; p-tau217 model: Adj. $R^2=0.32$); however, neither was predicted independently by plasma p-tau levels or Thal phase. Braak stage remained the significant predictor of cognitive measures for three of the four models. In the CDR model including plasma p-tau181, for every increase in Braak stage the model predicted 1 point higher on CDR sum of boxes (β -coefficient = 1.091 [0.024, 2.158], $p=0.045$). In the MMSE model including p-tau181, for every increase in Braak stage the model predicted nearly 1 point lower on MMSE (β -coefficient = -0.760 [-1.354, -0.166], $p=0.014$). The strongest model observed accounted for 32% of variability in MMSE and included plasma p-tau217, which found that for every increase in Braak stage the model predicted nearly 1 point lower on MMSE (β -coefficient = -0.667 [-1.293, -0.040], $p=0.038$).

Discussion

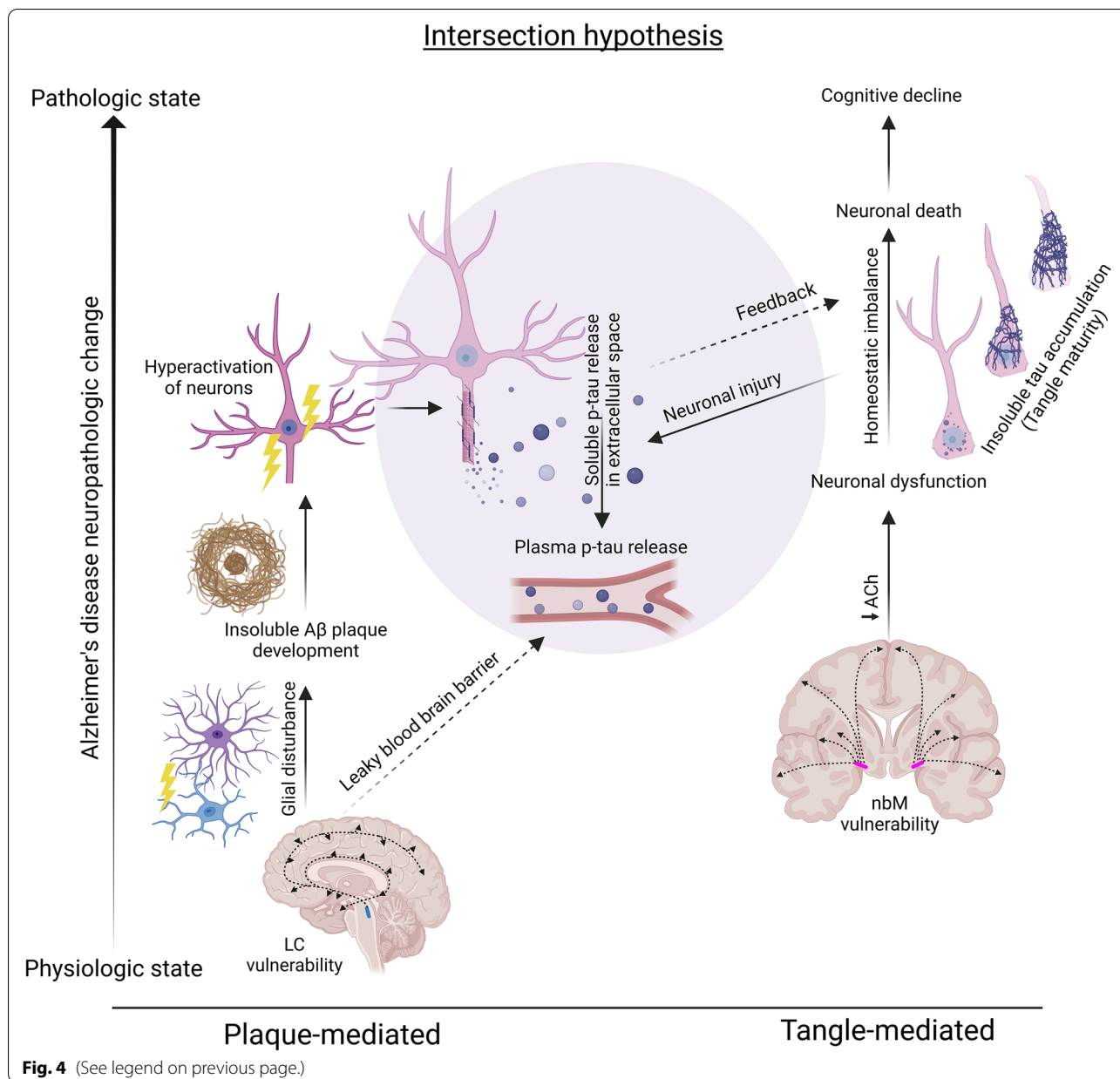
In this small series of 35 population-based autopsies from the Mayo Clinic Study of Aging, we report as much as 59% of the variability in plasma p-tau217 can be predicted by a combination of global neuropathologic scales. Tau and amyloid- β neuropathology remained significant predictors of plasma p-tau217, but not severity of LATE-NC stage or cerebrovascular disease scaled score. With as much as 31% of the variability accounted for in plasma p-tau181 levels by global neuropathologic scales, only amyloid- β remained the significant predictor. A common observation across each of the analyses performed

revealed plasma p-tau217 to have a stronger association with AD neuropathologic scales than p-tau181.

The neuropathologic findings in this study support the hypothesis that both tau and amyloid- β neuropathology intersect in their influence on plasma p-tau levels (Fig. 4). Interestingly, our study and others' provide supportive evidence that amyloid- β neuropathology has a stronger association with plasma p-tau levels than tau neuropathology [3, 8, 39]. To further extend the detailed work of Wennström and colleagues [49] that focused on the relationship between tau neuropathology and p-tau217, we compared both amyloid- β and tau neuropathology to plasma p-tau181 and p-tau217. Visual examination of this relationship using Thal phase [26] as a global amyloid- β scale demonstrated a biological influence potentially initiating between Thal phase 3 and Thal phase 4, suggesting either neuroanatomic extent to the brainstem or perhaps severity of amyloid- β plaque pathology may be required to cross a threshold. The relationship between regional amyloid- β burden measures from the parietal cortex was weaker than global Thal phase and did not indicate a linear increase in plasma p-tau levels as amyloid- β burden continued to increase in AD cases. Although amyloid- β plaque accumulation does not associate with cognitive decline when accounting for tau pathology [60, 61], supportive evidence suggests neuronal hyperactivation is mediated through an amyloid- β linked defect in synaptic transmission [51, 52]. Increased neuronal activity was previously shown to stimulate the release of tau in vitro, enhance tau pathology in vivo, and lead to production of amyloid- β [53, 54]. We speculate that amyloid- β induced hyperactivation of neurons may impact neuronal dysfunction sufficient to influence release of p-tau into

(See figure on next page.)

Fig. 4 Hypothesized intersection of amyloid- β and tau pathology in cortex and their influence on soluble p-tau release into plasma. We propose parallel processes occur for amyloid- β plaque (Left) and neurofibrillary tangle (Right) pathologies with an intersection (Middle) in the AD brain that impacts phospho-tau release into plasma. The hypothesized intersection is influenced by data from the cortex and may not apply to limbic regions, as the current study and others [49] observed a weaker relationship between limbic neuropathology and plasma p-tau levels. Plaque-mediated route: The locus coeruleus is highly vulnerable in the AD brain and is considered the earliest site of phospho-tau accumulation [50]. This noradrenergic hub nucleus (mid-sagittal brain, blue spot) sends projections throughout the brain [43] and is thought to influence amyloid- β plaque deposition through a mechanistic effect on glial disturbance [44]. Based upon available evidence that amyloid- β deposition induces a hyperactivation of neurons [51, 52], we speculate that the amyloid- β -mediated impact on soluble p-tau release is a result of increased neuronal activity that stimulates and enhances release of p-tau into the extracellular space [53, 54]. The association observed in the current study between lower locus coeruleus neuron counts and higher plasma p-tau levels is hypothesized to be mediated through noradrenergic deficiencies leading to increased leakage of blood-brain barrier [55] enhancing release of p-tau into plasma. Tangle-mediated route: The nucleus basalis of Meynert acts as a cholinergic hub (coronal brain, pink spot) that supplies acetylcholine to the cortex and is thought to influence cortical tangle accumulation through cholinergic deficiencies leading to neuronal dysfunction [45, 46, 56]. We did not observe an association between nucleus basalis of Meynert neuron count and plasma p-tau levels, which may suggest the resultant neuronal dysfunction from decreased acetylcholine does not affect p-tau release. The current study and others [4, 49] observed a strong relationship between severity of neurofibrillary tangle accumulation and plasma p-tau, which we speculate may result from neuronal injury [57] as tangles mature through their lifespan [58, 59]. Amyloid- β plaque accumulation does not associate with cognitive decline when accounting for tau pathology [60, 61], however we and others previously showed plasma p-tau to associate with cognitive decline [1, 3, 8, 9, 47, 48]. To evaluate both neuropathologic and soluble plasma p-tau contribution to cognitive decline, the current study utilized regression modeling. The results suggest that underlying tangle accumulation in the brain (Braak stage), but neither amyloid- β deposition (Thal phase) nor soluble plasma p-tau levels predict cognitive decline when modeled simultaneously. Acronyms: A β amyloid- β , AD Alzheimer's disease, LC locus coeruleus, nbM nucleus basalis of Meynert, p-tau phosphorylated tau, T threonine. Created with BioRender.com



the fluids without enough damage to impact cognitive decline.

Given the strength of the relationship between amyloid-β and plasma p-tau levels, we explored the novel hypothesis that neuronal loss in the locus coeruleus would associate with higher plasma p-tau levels. The locus coeruleus is a noradrenergic hub nucleus that sends projections throughout the brain and is thought to influence amyloid-β plaque deposition through a mechanistic effect on glial disturbance [43, 44]. Even in our small unselected series we observed a strong relationship between neuronal loss in the locus coeruleus and higher

p-tau181 and p-tau217 levels. The locus coeruleus is an area observed to develop neurofibrillary tangle pathology prior to entorhinal cortex [37, 62] that is currently being evaluated as an early AD biomarker [63, 64]. Furthermore, evidence from animal studies suggests damage to the locus coeruleus may impact cerebrovascular clearance mechanisms [55, 65]. We propose that the resultant increase in microvasculature permeability following locus coeruleus damage and amyloid-β-induced hyperexcitability of neurons may be the mechanism underlying the relationship between amyloid-β neuropathology and soluble p-tau release into plasma (Fig. 4).

Although we and others previously demonstrated a relationship between nucleus basalis of Meynert neuronal loss and cortical vulnerability to tangle pathology in AD [45, 46, 56, 66], we did not observe a relationship with p-tau plasma levels. We speculate that neuronal dysfunction related to impaired cholinergic projections may be insufficient to influence release of soluble p-tau into plasma. We did observe an association between Braak stage, a widely used global scale of tau pathology in the brain [25], and plasma p-tau levels. This confirms several reports demonstrating this robust association [9, 11, 39, 67]. A discernible threshold in p-tau levels was observed between Braak III and Braak IV, which corresponds with accumulation of cortical tau pathology by Braak IV [25, 37]. To further examine a more direct relationship with cortical severity, we immunostained tissue sections with pT181 and pT217 antibodies that recognize the same phosphorylation sites studied in plasma. Increasing immunohistochemical burden for both tau antibodies in AD cases appeared to have a ceiling effect without the observation of a linear increase in plasma p-tau levels. This supports data from a longitudinal study that stratified cases by Braak stage and observed a plasma p-tau181 ceiling effect [68]. Regional cortical tau burden had a stronger relationship with plasma p-tau levels than global Braak stage, which may reflect greater power to detect differences using quantitative methods over semi-quantitative global scales.

The association of hippocampal tau burden with both plasma p-tau181 and p-tau217 levels was modest in comparison to the strength of the relationship observed with either cortical tau or Braak stage. This supports prior work demonstrating higher correlation with cortical tau measures compared to medial temporal lobe structures using pT217 antibodies [49], and further confirms this relationship with pT181. As the hippocampus is a small region, p-tau levels may better reflect global involvement overrepresented by cortical tau load. An additional consideration for the weakened relationship in the hippocampus is that age-related tau accumulation in limbic structures that occurs independent of amyloid- β (i.e., primary age-related tauopathy [29]) may be insufficient to affect a discernible release of soluble p-tau into plasma [39]. We previously demonstrated that pT181 and pT217 antibodies recognize earlier aspects of tangle maturity [35], including pretangles and mature tangles. Thus, early tangle accumulation in the cortex may be more readily detected by the selected antibodies, enabling the observed relationship to be detected. In comparison, the hippocampus may have long-standing advanced tangle accumulation not as readily captured by the pT181 and pT217 antibodies.

We consistently observed a stronger relationship between neuropathologic measures and plasma p-tau217, compared to p-tau181. Moreover, the ratio between hippocampus to parietal cortex pT181 burden was muted in comparison to that observed in pT217. One possible explanation may be differences in antibody recognition of physiologic versus pathologic p-tau. Although uncommon, there were cases excluded from regional pT181 analyses as the immunohistochemical burden reflected axonal staining rather than tau pathology. A high-resolution quantitative proteomics study of tau demonstrated that phosphorylation at threonine 181 was observed in 70% of clinical controls with a Braak stage <IV and 92% of AD cases [69]. In comparison, phosphorylation at threonine 217 was observed in 14% of controls and 86% of AD cases [69]. These observations of physiologic differences between p-tau181 and p-tau217 should not detract from the prognostic data on p-tau181 [4, 6, 7, 9–11, 67], but may provide a deeper understanding of why p-tau217 associates more specifically with neuropathologic accumulation of tau pathology in the human brain.

Our study has several limitations that are important to consider, namely the small sample size. Although we investigated population-based study participants, all 35 participants who came to autopsy with plasma p-tau levels within 3 years were non-Hispanic white. With our finding that kidney health may impact plasma p-tau levels, further investigation in ethnically diverse cohorts remains critical as the prevalence of chronic kidney disease varies [70]. While our series had a range of neuropathologic diagnoses, small sample sizes precluded group comparisons. To offset this limitation, graphs are presented with visual representation of disease groups for interpretation of AD neuropathologic change (i.e., AD, pathological aging) in comparison with primary tauopathies (i.e., primary age-related tauopathy, argyrophilic grain disease, and progressive supranuclear palsy). To expand our understanding between neuropathologic changes and plasma p-tau levels, we utilized digital pathology methods. As a result, the 6F/3D amyloid- β antibody was used for evaluation as the 6E10 antibody labels intracellular APP and was expected to interfere with burden analysis. However, it should be noted that in some cases the 4G8 antibody may be more sensitive to diffuse plaque pathology [26, 71], which could have an effect on performing Thal phase with 6F/3D. Our quantitative digital pathology studies were only performed in the CA1-subiculum of the hippocampus and parietal cortex, which may limit interpretation with other brain regions. Most of our cases were older than

75 years at death, therefore limiting our interpretation in younger autopsy cohorts. We did not observe a relationship between age at plasma draw and plasma p-tau levels, but more work is needed in younger cases to see if this remains a consistent finding.

Conclusions

Our findings provide strong evidence that soluble plasma p-tau levels reflect insoluble accumulation of amyloid- β and tau pathology. As cut-points for diagnostic utility continue to undergo determination, it is important to note that plasma p-tau negativity does not exclude for the possibility of underlying tau and amyloid- β pathology. Instead, plasma p-tau positivity will reflect a threshold crossed where p-tau levels correspond to a functional measure ascribed to significant disease-relevant changes. We propose parallel processes occur for amyloid- β deposits and tangle development with an intersection between these neuropathologies in AD that impacts soluble p-tau release, but not necessarily cortical tangle accumulation. The association observed between locus coeruleus and plasma p-tau levels suggests noradrenergic deficiencies may play a role in release of tau that we hypothesize to be mediated through amyloid- β -induced hyperactivation of neurons and increased microvasculature leakage.

Abbreviations

AD: Alzheimer's disease; AGD: Argyrophilic grain disease; ALT: Alanine transaminase; AST: Aspartate aminotransferase; AUC: Area under the curves; CDR: Clinical Dementia Rating; CERAD: Consortium to Establish a Registry for Alzheimer's Disease; IQR: Interquartile range; LATE-NC: Limbic-predominant age-related TDP-43 encephalopathy neuropathologic change; MCSA: Mayo Clinic Study of Aging; MMSE: Mini-Mental State Examination; MSD: Meso scale discovery; PART: Primary age-related tauopathy; PET: Positron emission tomography; p-tau: Phosphorylated-tau; p-tau181: Phosphorylated-tau at threonine 181; p-tau217: Phosphorylated-tau at threonine 217; REP: Rochester Epidemiology Project; ROC: Receiver operating characteristic; SUVr: Standardized uptake value ratios; TDP-43: TAR DNA binding protein 43.

Supplementary Information

The online version contains supplementary material available at <https://doi.org/10.1186/s13024-022-00578-0>.

Additional file 1.

Acknowledgements

We thank Monica Castaneda-Casey and Virginia Phillips for their dedication and support. We are grateful to the patients and their families for their generous brain donations to help further our knowledge of Alzheimer's disease. Programmatic support by Sabrina Rothberg and Kelsey Caetano-Anolles continues to be invaluable, and we are appreciative of their dedication.

Authors' contributions

MEM and MMM designed the study and performed primary interpretation of the data. MEM wrote the manuscript, with MMM, JLD, and CRJ Jr. contributing substantial edits. RCP, CRJ Jr., DSK, PV, JGR were responsible for acquisition

of clinical data. MEM, ATN, RRR, and DWD were responsible for acquisition of neuropathology data. MEM, CMM, DMR, JFT, TNHS were responsible for neurohistology organization and digital pathology analyses. MEM, BDCB, JLD, MMM were responsible for interpretation of plasma p-tau data. NK performed Kalaria cerebrovascular disease scoring. NK and BJM evaluated TDP-43 pathology. ATN, RRR, and DWD were responsible for neuropathologic examination. JAS performed statistical analyses. Funding was obtained by MEM, RCP, PV, JGR, MMM. All authors contributed and critically reviewed the final version of the manuscript. All authors read and approved the final manuscript.

Funding

The investigators are supported by grants from National Institute of Health/ National Institute on Aging (R01 AG054449, R01 AG073282, R01 AG075802, P30 AG062677, R01 AG034676, RF1 AG069052, U01 AG057195, U01 AG006786, R37 AG011378, P50 AG16574), and the GHR Foundation.

Availability of data and materials

All requests for raw and analyzed data and related materials will be reviewed by Mayo Clinic's Legal Department and Mayo Clinic Ventures to verify whether each request is subject to any intellectual property or confidentiality obligations. Requests for patient-related data not included in the paper will not be considered. Any data and materials that can be shared will be released via a Data Use/Share Agreement or Material Transfer Agreement.

Declarations

Ethics approval and consent to participate

The Mayo Clinic and Olmsted Medical Center Institutional Review Boards approved this study. All participants provided written informed consent.

Consent for publication

Not applicable.

Competing interests

MEM is a consultant for AVID Radiopharmaceuticals. She receives support from the NIH/NIA and State of Florida. VJL serves as consultant for Bayer Schering Pharma, Philips Molecular Imaging, Piramal Imaging, AVID Radiopharmaceuticals, Eisai Inc., and GE Healthcare and receives research support from GE Healthcare, Siemens Molecular Imaging, AVID Radiopharmaceuticals, the NIH (NIA, NCI), and the MN Partnership for Biotechnology and Medical Genomics. JLD was previously an employee and stockholder of Eli Lilly and Company. RCP serves as a consultant for Biogen, Inc., Roche, Inc., Merck, Inc., Genentech Inc. (DSMB), Nestle, Inc., and Eisai, Inc., receives publishing royalties from Mild Cognitive Impairment (Oxford University Press, 2003), and UpToDate. CRJ serves on an independent data monitoring board for Roche, has served as a speaker for Eisai, and consulted for Biogen, but he receives no personal compensation from any commercial entity. He receives research support from NIH and the Alexander Family Alzheimer's Disease Research Professorship of the Mayo Clinic. DSK serves on a Data Safety Monitoring Board for the DIAN study. He served on a Data Safety monitoring Board for a tau therapeutic for Biogen, but receives no personal compensation. He is a site investigator in the Biogen aducanumab trials. He is an investigator in a clinical trial sponsored by Lilly Pharmaceuticals and the University of Southern California. He serves as a consultant for Samus Therapeutics, Roche and Alzeca Biosciences but receives no personal compensation. PV received speaker fees from Miller Medical Communications, Inc. and receives research support from the NIH. JGR serves on the editorial board for *Neurology* and receives research support from the NIH. MMM consulted for Biogen and Brain Protection Company and receives funding from the NIH/NIA and DOD.

Author details

¹Department of Neuroscience, Mayo Clinic Florida, 4500 San Pablo Road, Jacksonville, FL 32224, USA. ²Department of Quantitative Health Sciences, Mayo Clinic, Rochester, MN, USA. ³Department of Laboratory Medicine and Pathology, Mayo Clinic, Rochester, MN, USA. ⁴Department of Radiology, Mayo Clinic, Rochester, MN, USA. ⁵Department of Neurology, Indiana University, Indianapolis, IN, USA. ⁶Department of Neurology, Mayo Clinic, Rochester, MN, USA. ⁷Wake Forest University School of Medicine, Winston-Salem, NC, USA. ⁸Department of Epidemiology and Prevention, Division of Public Health

Sciences, Wake Forest University School of Medicine, 525 Vine, 5th floor, Winston-Salem, NC 27157, USA.

Received: 24 May 2022 Accepted: 26 October 2022

Published online: 27 December 2022

References

- Karikari TK, Pascoal TA, Ashton NJ, Janelidze S, Benedet AL, Rodriguez JL, et al. Blood phosphorylated tau 181 as a biomarker for Alzheimer's disease: a diagnostic performance and prediction modelling study using data from four prospective cohorts. *Lancet Neurol*. 2020;19:422–33.
- Teunissen CE, Verberk IMW, Thijssen EH, Vermunt L, Hansson O, Zetterberg H, et al. Blood-based biomarkers for Alzheimer's disease: towards clinical implementation. *Lancet Neurol*. 2022;21:66–77.
- Mielke MM, Hagen CE, Xu J, Chai X, Vemuri P, Lowe VJ, et al. Plasma phospho-tau181 increases with Alzheimer's disease clinical severity and is associated with tau- and amyloid-positron emission tomography. *Alzheimers Dement*. 2018;14:989–97.
- Palmqvist S, Janelidze S, Quiroz YT, Zetterberg H, Lopera F, Stomrud E, et al. Discriminative Accuracy of Plasma Phospho-tau217 for Alzheimer Disease vs Other Neurodegenerative Disorders. *JAMA*. 2020;324:772–81.
- Ashton NJ, Leuzy A, Karikari TK, Mattsson-Carlgen N, Dodich A, Boccardi M, et al. The validation status of blood biomarkers of amyloid and phospho-tau assessed with the 5-phase development framework for AD biomarkers. *Eur J Nucl Med Mol Imaging*. 2021;48:2140–56.
- Brickman AM, Manly JJ, Honig LS, Sanchez D, Reyes-Dumeyer D, Lantigua RA, et al. Plasma p-tau181, p-tau217, and other blood-based Alzheimer's disease biomarkers in a multi-ethnic, community study. *Alzheimers Dement*. 2021;17:1353–64.
- Janelidze S, Mattsson N, Palmqvist S, Smith R, Beach TG, Serrano GE, et al. Plasma P-tau181 in Alzheimer's disease: relationship to other biomarkers, differential diagnosis, neuropathology and longitudinal progression to Alzheimer's dementia. *Nat Med*. 2020;26:379–86.
- Thijssen EH, La Joie R, Strom A, Fonseca C, Iaccarino L, Wolf A, et al. Plasma phosphorylated tau 217 and phosphorylated tau 181 as biomarkers in Alzheimer's disease and frontotemporal lobar degeneration: a retrospective diagnostic performance study. *Lancet Neurol*. 2021;20:739–52.
- Lantero Rodriguez J, Karikari TK, Suarez-Calvet M, Troakes C, King A, Emersic A, et al. Plasma p-tau181 accurately predicts Alzheimer's disease pathology at least 8 years prior to post-mortem and improves the clinical characterisation of cognitive decline. *Acta Neuropathol*. 2020;140:267–78.
- Thijssen EH, La Joie R, Wolf A, Strom A, Wang P, Iaccarino L, et al. Diagnostic value of plasma phosphorylated tau181 in Alzheimer's disease and frontotemporal lobar degeneration. *Nat Med*. 2020;26:387–97.
- Ashton NJ, Pascoal TA, Karikari TK, Benedet AL, Lantero-Rodriguez J, Brinkmalm G, et al. Plasma p-tau231: a new biomarker for incipient Alzheimer's disease pathology. *Acta Neuropathol*. 2021;141(5):709–24.
- Sato C, Barthelemy NR, Mawuenyega KG, Patterson BW, Gordon BA, Jockel-Balsarotti J, et al. Tau Kinetics in Neurons and the Human Central Nervous System. *Neuron*. 2018;97:1284–98 e1287.
- Risacher SL, Fandos N, Romero J, Sherriff I, Pesini P, Saykin AJ, et al. Plasma amyloid beta levels are associated with cerebral amyloid and tau deposition. *Alzheimers Dement (Amst)*. 2019;11:510–9.
- Mielke MM, Dage JL, Frank RD, Algeciras-Schimmich A, Knopman DS, Lowe VJ, et al. Performance of plasma phosphorylated tau 181 and 217 in the community. *Nat Med*. 2022;28(7):1398–405. <https://doi.org/10.1038/s41591-022-01822-2>.
- Deramecourt V, Slade JY, Oakley AE, Perry RH, Ince PG, Maurage CA, et al. Staging and natural history of cerebrovascular pathology in dementia. *Neurology*. 2012;78:1043–50.
- Nelson PT, Dickson DW, Trojanowski JQ, Jack CR, Boyle PA, Arfanakis K, et al. Limbic-predominant age-related TDP-43 encephalopathy (LATE): consensus working group report. *Brain*. 2019;142:1503–27.
- Roberts RO, Geda YE, Knopman DS, Cha RH, Pankratz VS, Boeve BF, et al. The Mayo Clinic Study of Aging: design and sampling, participation, baseline measures and sample characteristics. *Neuroepidemiology*. 2008;30:58–69.
- Morris JC. The Clinical Dementia Rating (CDR): current version and scoring rules. *Neurology*. 1993;43:2412–4.
- Folstein MF, Folstein SE, McHugh PR. "Mini-mental state": A practical method for grading the cognitive state of patients for the clinician. *J Psychiatr Res*. 1975;12:189–98.
- Mielke MM, Frank RD, Dage JL, Jeromin A, Ashton NJ, Blennow K, et al. Comparison of Plasma Phosphorylated Tau Species With Amyloid and Tau Positron Emission Tomography, Neurodegeneration, Vascular Pathology, and Cognitive Outcomes. *JAMA Neurol*. 2021;78:1108–17.
- Mirra SS, Heyman A, McKeel D, Sumi S, Crain BJ, Brownlee L, et al. The Consortium to Establish a Registry for Alzheimer's Disease (CERAD): Part II. Standardization of the neuropathologic assessment of Alzheimer's disease. *Neurology*. 1991;41:479.
- Montine TJ, Phelps CH, Beach TG, Bigio EH, Cairns NJ, Dickson DW, et al. National Institute on Aging-Alzheimer's Association guidelines for the neuropathologic assessment of Alzheimer's disease: a practical approach. *Acta Neuropathol*. 2012;123:1–11.
- McKeith IG, et al. Diagnosis and management of dementia with Lewy bodies 4th consensus report of the DLB consortium. *Neurology*. 2016; In Press.
- Mackenzie IR, Neumann M, Baborie A, Sampathu DM, Du Plessis D, Jaros E, et al. A harmonized classification system for FTLTDP pathology. *Acta Neuropathol*. 2011;122:111–3.
- Braak H, Braak E. Neuropathological staging of Alzheimer-related changes. *Acta Neuropathol*. 1991;82:239–59.
- Thal DR, Rub U, Orantes M, Braak H. Phases of A beta-deposition in the human brain and its relevance for the development of AD. *Neurology*. 2002;58:1791–800.
- Hauw JJ, Daniel SE, Dickson D, Horoupian DS, Jellinger K, Lantos PL, et al. Preliminary NINDS neuropathologic criteria for Steele-Richardson-Olszewski syndrome (progressive supranuclear palsy). *Neurology*. 1994;44:2015–9.
- Ferrer I, Santpere G, van Leeuwen FW. Argyrophilic grain disease. *Brain*. 2008;131:1416–32.
- Crary JF, Trojanowski JQ, Schneider JA, Abisambra JF, Abner EL, Alafuzoff I, et al. Primary age-related tauopathy (PART): a common pathology associated with human aging. *Acta Neuropathol*. 2014;128:755–66.
- Murray ME, Dickson DW. Is pathological aging a successful resistance against amyloid-beta or preclinical Alzheimer's disease? *Alzheimers Res Ther*. 2014;6:24.
- Dickson DW, Crystal HA, Mattiace LA, Masur DM, Blau AD, Davies P, et al. Identification of normal and pathological aging in prospectively studied nondemented elderly humans. *Neurobiol Aging*. 1992;13:179–89.
- Lowe VJ, Curran G, Fang P, Liesinger AM, Josephs KA, Parisi JE, et al. An autoradiographic evaluation of AV-1451 Tau PET in dementia. *Acta Neuropathol Commun*. 2016;4:58.
- Lowe VJ, Lundt ES, Albertson SM, Min HK, Fang P, Przybelski SA, et al. Tau-positron emission tomography correlates with neuropathology findings. *Alzheimers Dement*. 2020;16:561–71.
- Ishizawa T, Ko LW, Cookson N, Davies P, Espinoza M, Dickson DW. Selective neurofibrillary degeneration of the hippocampal CA2 sector is associated with four-repeat tauopathies. *J Neuropathol Exp Neurol*. 2002;61:1040–7.
- Moloney CM, Labuzan SA, Crook JE, Siddiqui H, Castanedes-Casey M, Lachner C, et al. Phosphorylated tau sites that are elevated in Alzheimer's disease fluid biomarkers are visualized in early neurofibrillary tangle maturity levels in the post mortem brain. *Alzheimers Dement*. 2022. Advance online publication. <https://doi.org/10.1002/alz.12749>.
- Nho K, Kueider-Paisley A, Ahmad S, MahmoudianDehkordi S, Arnold M, Risacher SL, et al. Association of Altered Liver Enzymes With Alzheimer Disease Diagnosis, Cognition, Neuroimaging Measures, and Cerebrospinal Fluid Biomarkers. *JAMA Netw Open*. 2019;2:e197978.
- Braak H, Thal DR, Ghebremedhin E, Del Tredici K. Stages of the pathologic process in Alzheimer disease: age categories from 1 to 100 years. *J Neuropathol Exp Neurol*. 2011;70:960–9.
- Shcherbinin S, Evans CD, Lu M, et al. Association of Amyloid Reduction After Donanemab Treatment With Tau Pathology and Clinical Outcomes: The TRAILBLAZER-ALZ Randomized Clinical Trial. *JAMA Neurol*. 2022;79(10):1015–1024. doi:10.1001/jamaneuro.2022.2793
- Mattsson-Carlgen N, Janelidze S, Bateman RJ, Smith R, Stomrud E, Serrano GE, et al. Soluble P-tau217 reflects amyloid and tau pathology

- and mediates the association of amyloid with tau. *EMBO Mol Med*. 2021;13:e14022.
40. Robinson JL, Lee EB, Xie SX, Rennert L, Suh E, Bredenberg C, et al. Neurodegenerative disease concomitant proteinopathies are prevalent, age-related and APOE4-associated. *Brain*. 2018;141:2181–93.
 41. Schneider JA, Arvanitakis Z, Bang W, Bennett DA. Mixed brain pathologies account for most dementia cases in community-dwelling older persons. *Neurology*. 2007;69:2197–204.
 42. Nguyen AT, Kouri N, Labuzan SA, Przybelski SA, Lesnick TG, Raghavan S, et al. Neuropathologic scales of cerebrovascular disease associated with diffusion changes on MRI. *Acta Neuropathol*. 2022;144(6):1117–25.
 43. Matchett BJ, Grinberg LT, Theofilas P, Murray ME. The mechanistic link between selective vulnerability of the locus coeruleus and neurodegeneration in Alzheimer's disease. *Acta Neuropathol*. 2021;141:631–50.
 44. Heneka MT, Nadrigny F, Regen T, Martinez-Hernandez A, Dumitrescu-Ozimek L, Terwel D, et al. Locus coeruleus controls Alzheimer's disease pathology by modulating microglial functions through norepinephrine. *Proc Natl Acad Sci U S A*. 2010;107:6058–63.
 45. Hanna Al-Shaikh FS, Duara R, Crook JE, Lesser ER, Schaefferbeke J, Hinkle KM, et al. Selective Vulnerability of the Nucleus Basalis of Meynert Among Neuropathologic Subtypes of Alzheimer Disease. *JAMA Neurol*. 2020;77(2):225–33. <https://doi.org/10.1001/jamaneurol.2019.3606>.
 46. Mesulam MM. Cholinergic circuitry of the human nucleus basalis and its fate in Alzheimer's disease. *J Comp Neurol*. 2013;521:4124–44.
 47. Chhatwal JP, Schultz AP, Dang Y, Ostaszewski B, Liu L, Yang HS, et al. Plasma N-terminal tau fragment levels predict future cognitive decline and neurodegeneration in healthy elderly individuals. *Nat Commun*. 2020;11:6024.
 48. Mila-Aloma M, Ashton NJ, Shekari M, Salvado G, Ortiz-Romero P, Montoliu-Gaya L, et al. Plasma p-tau231 and p-tau217 as state markers of amyloid-beta pathology in preclinical Alzheimer's disease. *Nat Med*. 2022;28:1797–801.
 49. Wennstrom M, Janelidze S, Nilsson KPR, Netherlands Brain B, Serrano GE, Beach TG, et al. Cellular localization of p-tau217 in brain and its association with p-tau217 plasma levels. *Acta Neuropathol Commun*. 2022;10:3.
 50. Braak H, Del Tredici K. The pathological process underlying Alzheimer's disease in individuals under thirty. *Acta Neuropathol*. 2011;121:171–81.
 51. Busche MA, Eichhoff G, Adelsberger H, Abramowski D, Wiederhold KH, Haass C, et al. Clusters of hyperactive neurons near amyloid plaques in a mouse model of Alzheimer's disease. *Science*. 2008;321:1686–9.
 52. Zott B, Simon MM, Hong W, Unger F, Chen-Engerer HJ, Frosch MP, et al. A vicious cycle of beta amyloid-dependent neuronal hyperactivation. *Science*. 2019;365:559–65.
 53. Palop JJ, Mucke L. Amyloid-beta-induced neuronal dysfunction in Alzheimer's disease: from synapses toward neural networks. *Nat Neurosci*. 2010;13:812–8.
 54. Wu JW, Hussaini SA, Bastille IM, Rodriguez GA, Mrejeru A, Rilett K, et al. Neuronal activity enhances tau propagation and tau pathology in vivo. *Nat Neurosci*. 2016;19:1085–92.
 55. Kelly SC, McKay EC, Beck JS, Collier TJ, Dorrance AM, Counts SE. Locus Coeruleus Degeneration Induces Forebrain Vascular Pathology in a Transgenic Rat Model of Alzheimer's Disease. *J Alzheimers Dis*. 2019;70:369–86.
 56. Tiernan CT, Ginsberg SD, He B, Ward SM, Guillozet-Bongaarts AL, Kanaan NM, et al. Pretangle pathology within cholinergic nucleus basalis neurons coincides with neurotrophic and neurotransmitter receptor gene dysregulation during the progression of Alzheimer's disease. *Neurobiol Dis*. 2018;117:125–36.
 57. Yanamandra K, Patel TK, Jiang H, Schindler S, Ulrich JD, Boxer AL, et al. Anti-tau antibody administration increases plasma tau in transgenic mice and patients with tauopathy. *Sci Transl Med*. 2017;9:eaal2029.
 58. Moloney CM, Labuzan SA, Crook JE, Siddiqui H, Castanedes-Casey M, Lachner C, et al. Phosphorylated tau sites that are elevated in Alzheimer's disease fluid biomarkers are visualized in early neurofibrillary tangle maturity levels in the post mortem brain. *Alzheimers Dement*. 2022; Online ahead of print.
 59. Moloney CM, Lowe VJ, Murray ME. Visualization of neurofibrillary tangle maturity in Alzheimer's disease: A clinicopathologic perspective for biomarker research. *Alzheimers Dement*. 2021;17(9):1554–74.
 60. Murray ME, Lowe VJ, Graff-Radford NR, Liesinger AM, Cannon A, Przybelski SA, et al. Clinicopathologic and 11C-Pittsburgh compound B implications of Thal amyloid phase across the Alzheimer's disease spectrum. *Brain*. 2015;138:1370–81.
 61. Nelson PT, Alafuzoff I, Bigio EH, Bouras C, Braak H, Cairns NJ, et al. Correlation of Alzheimer disease neuropathologic changes with cognitive status: a review of the literature. *J Neuropathol Exp Neurol*. 2012;71:362–81.
 62. Arendt T, Bruckner MK, Morawski M, Jager C, Gertz HJ. Early neurone loss in Alzheimer's disease: cortical or subcortical? *Acta Neuropathol Commun*. 2015;3:10.
 63. Jacobs HIL, Becker JA, Kwong K, Engels-Dominguez N, Prokopiou PC, Papp KV, et al. In vivo and neuropathology data support locus coeruleus integrity as indicator of Alzheimer's disease pathology and cognitive decline. *Sci Transl Med*. 2021;13:eabj2511.
 64. Chu WT, Wang WE, Zaborszky L, Golde TE, De Kosky S, Duara R, et al. Association of Cognitive Impairment With Free Water in the Nucleus Basalis of Meynert and Locus Coeruleus to Transentorhinal Cortex Tract. *Neurology*. 2022;98:e700–10.
 65. Kalinin S, Gavriluyk V, Polak PE, Vasser R, Zhao J, Heneka MT, et al. Noradrenaline deficiency in brain increases beta-amyloid plaque burden in an animal model of Alzheimer's disease. *Neurobiol Aging*. 2007;28:1206–14.
 66. Lin CP, Frigerio I, Boon BDC, Zhou Z, Rozemuller AJM, Bouwman FH, et al. Structural (dys)connectivity associates with cholinergic cell density in Alzheimer's disease. *Brain*. 2022;145:2869–81.
 67. Grothe MJ, Moscoso A, Ashton NJ, Karikari TK, Lantero-Rodriguez J, Snellman A, et al. Associations of Fully Automated CSF and Novel Plasma Biomarkers With Alzheimer Disease Neuropathology at Autopsy. *Neurology*. 2021;97(12):e1229–42.
 68. La Joie R, Ayakta N, Seeley WW, Borys E, Boxer AL, DeCarli C, et al. Multisite study of the relationships between antemortem [(11)C]PIB-PET Centiloid values and postmortem measures of Alzheimer's disease neuropathology. *Alzheimers Dement*. 2019;15:205–16.
 69. Wesseling H, Mair W, Kumar M, Schlawfer CN, Tang S, Beerepoot P, et al. Tau PTM Profiles Identify Patient Heterogeneity and Stages of Alzheimer's Disease. *Cell*. 2020;183:1699–713 e1613.
 70. Peralta CA, Katz R, DeBoer I, Ix J, Sarnak M, Kramer H, et al. Racial and ethnic differences in kidney function decline among persons without chronic kidney disease. *J Am Soc Nephrol*. 2011;22:1327–34.
 71. Alafuzoff I, Pikkarainen M, Arzberger T, Thal DR, Al-Sarraj S, Bell J, et al. Inter-laboratory comparison of neuropathological assessments of beta-amyloid protein: a study of the BrainNet Europe consortium. *Acta Neuropathol*. 2008;115:533–46.

Publisher's Note

Springer Nature remains neutral with regard to jurisdictional claims in published maps and institutional affiliations.

Ready to submit your research? Choose BMC and benefit from:

- fast, convenient online submission
- thorough peer review by experienced researchers in your field
- rapid publication on acceptance
- support for research data, including large and complex data types
- gold Open Access which fosters wider collaboration and increased citations
- maximum visibility for your research: over 100M website views per year

At BMC, research is always in progress.

Learn more biomedcentral.com/submissions

